Removal of Microparticles by Ciliated Surfaces-an Experimental Study

Zhang, Shuaizhong; Wang, Ye; Onck, Patrick R.; den Toonder, Jaap M. J.

IMPORTANT NOTE: You are advised to consult the publisher's version (publisher's PDF) if you wish to cite from it. Please check the document version below.

Document Version
Publisher's PDF, also known as Version of record

Publication date:
2019

Link to publication in University of Groningen/UMCG research database

Removal of Microparticles by Ciliated Surfaces—an Experimental Study

Shuaizhong Zhang, Ye Wang, Patrick R. Onck, and Jaap M. J. den Toonder*

Biological cilia are versatile hair-like organelles that are very efficient in manipulating particles for, e.g., feeding, antifouling, and cell transport. Inspired by the versatility of cilia, this paper experimentally demonstrates active particle-removal by self-cleaning surfaces that are fully or partially covered with micromolded magnetic artificial cilia (MAC). Actuated by a rotating magnet, the MAC can perform a tilted conical motion, which leads to the removal of spherical particles of different sizes in water, as well as irregular-shaped sand grains both in water and in air. These findings can contribute to the development of novel particulate manipulation and self-cleaning/antifouling surfaces, which can be applied, e.g., to prevent fouling of (bio)sensors in lab-on-a-chip devices, and to prevent biofouling of submerged surfaces such as marine sensors and water quality analyzers.

1. Introduction

The fouling of surfaces submerged in a liquid is an important problem for many applications.[1] A specific example is the accumulation of microparticles in lab-on-a-chip devices, which for instance can clog the microchannels, or interfere with detection by contaminating sensor surfaces.[1i] Classical chip cleaning protocols are tedious and time consuming, or they disrupt the ongoing experiments. Another example is the biofouling of submerged surfaces such as marine sensors,[2] water quality analyzers, off-shore structures and ship hulls which is a serious problem due to many factors including i) the vast biodiversity in fouling species, ii) the broad range of attachment behaviors and adhesion mechanisms, and iii) geographical and seasonal differences. Nowadays, antifouling strategies are based on either chemical or physical mechanisms, which, however, cannot deter the settlement

and attachment of the whole vast variety of biofouling agents.[3] One biologically inspired strategy to tackle this problem is through cilia-induced particle manipulation and cleaning.[4] Biological cilia are slender microscopic hair-like protrusions of cells with a typical length between 2 and 15 µm, which were first reported by Antony van Leeuwenhoek in 1675,[5] and have been found to exist ubiquitously in nature.[6] For example, 1) immotile cilia exist in the cochlear, the inner ear, sensing sound and gravity[7]; 2) motile cilia cover the outer surface of a paramecium, an aquatic micro-organism, functioning as actuators that propel the creature through water[7]; 3) motile cilia line the windpipe and the lungs of the human body, helping to clean up mucus and dust out of the respiratory tract[4a,b]; 4) motile cilia line the inner walls of the fallopian tubes, transporting egg cells to the uterus[4b,c]; 5) cilia grow in the mouth of some marine suspension microorganisms, facilitating feeding[4d-k]; 6) cilia cover the outer surfaces of mollusks and coral, and their continuous motion shields away sand and fouling organisms.[4l-n] Inspired by this versatile cellular organelle, researchers have studied especially the possibility of employing artificial cilia as a means to transport and mix fluids.[8] Recently, investigations to use artificial cilia to manipulate particles and create antifouling surfaces have been carried out, mostly using numerical computations.[9] Simulations have demonstrated that both active and passive artificial cilia can be harnessed to repel neutrally buoyant spherical microparticles in their vicinity.[9g-i] Experimental studies have shown that magnetic surfaces featured with cilia-resembling micropillars can transport a drop of water.[9k,l] However, there is no experimental work that shows particle removal and antifouling of ciliated surfaces in practice. To bring the concept of antifouling by ciliated surfaces closer to real life applications, it is therefore important to perform experiments that demonstrate this capacity of artificial cilia—this is the topic of the current paper.

As a proof-of-principle, we experimentally demonstrate for the first time that active cilia actuated by a rotating magnet have the capacity to remove a large size range of microparticles (representing fouling agents or cells) from ciliated areas. We studied the impact of the motion of the magnetic artificial cilia (MAC), the actuation frequency and the arrangement of the MAC on the repelling efficiency of microparticles. The results show that over 95% of the microparticles present within the ciliated area can be removed within 1 min when

S. Z. Zhang, Dr. Y. Wang, Prof. J. M. J. den Toonder
Department of Mechanical Engineering
Eindhoven University of Technology
P.O. Box 513, 5600 MB Eindhoven, The Netherlands
E-mail: J.M.J.d.Toonder@tue.nl
S. Z. Zhang, Dr. Y. Wang, Prof. J. M. J. den Toonder
Institute for Complex Molecular Systems
Eindhoven University of Technology
5600 MB Eindhoven, The Netherlands
Prof. P. R. Onck
Zernike Institute for Advanced Materials
University of Groningen
NL-9700 AE Groningen, The Netherlands

The ORCID identification number(s) for the author(s) of this article can be found under https://doi.org/10.1002/adfm.201806434.
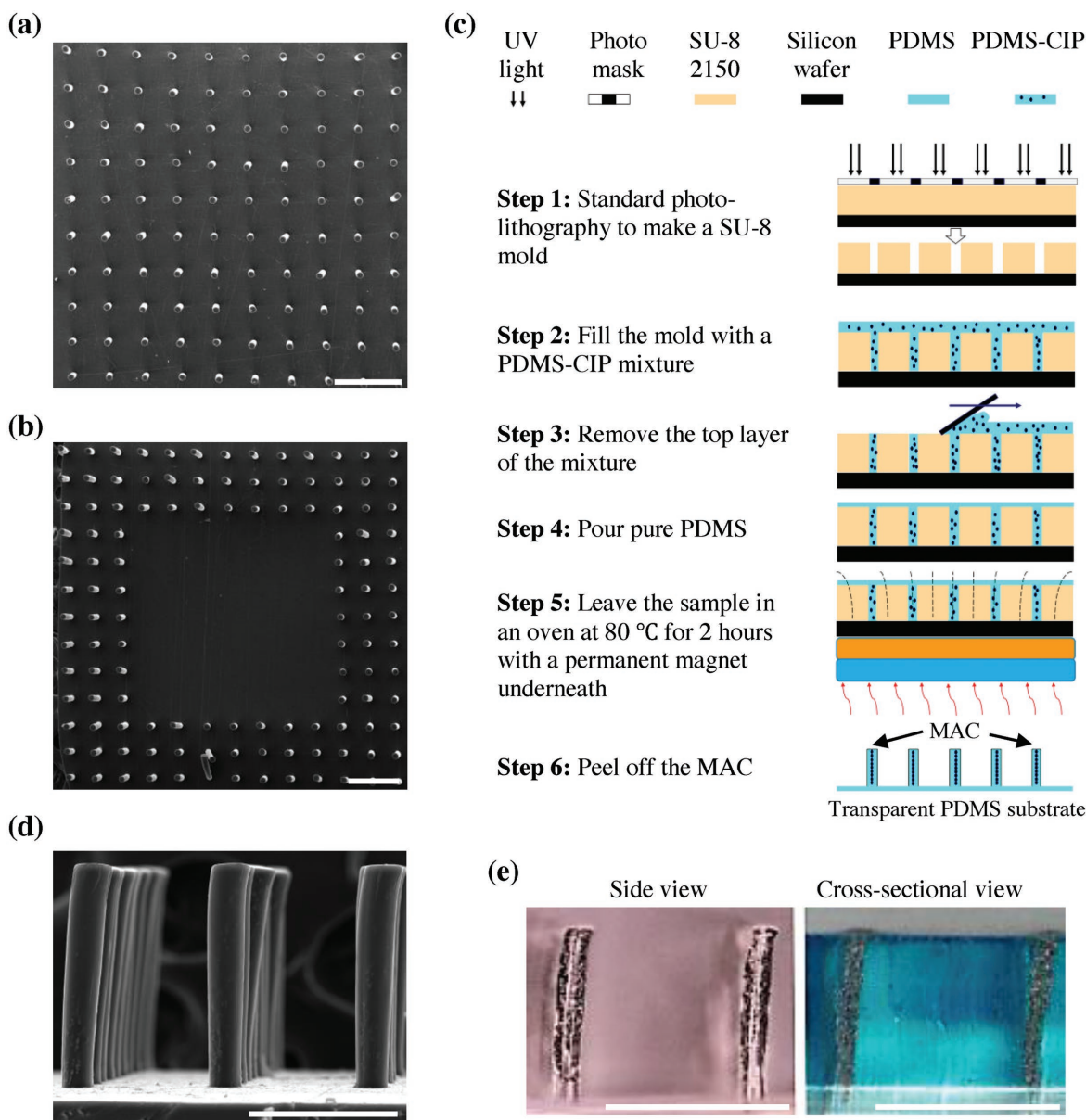
Figure 1. Fabrication scheme and microscopy images of the fabricated cilia. Top-view SEM images of a) a "fully ciliated surface" covered with orthogonally arranged MAC in a square array of 10 × 10 = 100 cilia and b) a "partially ciliated surface" consisting of a central unciliated area surrounded by three lines of MAC. The MAC have a diameter of 50 μm, a height of 350 μm, and a pitch of 250 μm. The scale bars are 500 μm. c) Schematics of the fabrication process of the MAC. The illustration is not to scale. d) A side-view SEM image of the MAC, with a diameter, a height, and a pitch of 50, 350, and 250 μm, respectively. The scale bar is 250 μm. e) Optical microscopy images of the MAC at both side view and cross-sectional view. The scale bars are 350 μm. Panels (c) and (e) are reproduced with permission.[8h] Copyright 2018, Elsevier B.V.

the MAC perform an inclined tilted conical motion rotating at 40 Hz. Moreover, MAC arranged around a bare unciliated central region are shown to be able to remove all particles from that region. These findings demonstrate that our ciliated surfaces are capable of creating a particle-free clean surface area, which may have relevant applications in lab-on-a-chip, marine biofouling, and possibly also particle manipulation including sorting and collecting. In addition, our work also offers new insights into the physical factors that enable the antifouling and feeding of marine organisms.[4d-n]

2. Results and Discussion

2.1. Ciliated Surfaces and Actuation Scheme

The particle-removal capability of two types of ciliated surfaces were studied: i) a surface covered with orthogonally arranged MAC in a square array of 10 × 10 = 100 cilia (**Figure 1**a), termed "fully ciliated surface"; ii) a surface consisting of a central unciliated square region surrounded by three rows of MAC on each side (Figure 1b), termed "partially ciliated surface." One primary

**ADVANCED
SCIENCE NEWS**
www.advancedsciencenews.com

**ADVANCED
FUNCTIONAL
MATERIALS**
www.afm-journal.de

reason to study the partially ciliated surface is that for certain applications, e.g., an optical sensor, anything covering the sensor surface may disrupt the detection—in such case rows of cilia surrounding the sensor area may be useful for antifouling.[2] The MAC were fabricated using a facile and reproducible micromolding process (Figure 1c). Scanning electron microscopy (SEM) images (Figure 1a,b,d) confirm the cylindrical shape of the MAC which have a diameter of 50 µm and a height of 350 µm. By fabricating molds featured with microwells of different pitches, MAC with variable pitches of 250, 350, and 450 µm, respectively, were molded. Bright-field microscopy images (Figure 1e) show that the magnetic particles are linearly aligned along the long axis of the cilia. The MAC with such a magnetic particle distribution were previously verified to have superior magnetic susceptibility and actuation properties compared to the MAC with a random internal magnetic particle distribution, and were able to generate substantial fluid flow in a microfluidic channel network.[8h] The magnetic properties and the bending performance of the artificial cilia were reported in our earlier paper.[8h]

The ciliated surfaces were integrated in a microfluidic chip with an open-top circular channel with a rectangular cross section with a channel width of 5 mm and channel height of 4 mm (**Figure 2**a,b). The MAC were actuated externally by a homebuilt magnetic setup as shown in Figure 2c. The vertical distance h between the top surface of the magnet and the MAC was set to 2 mm. The motion of the MAC can be tuned by changing r and d, as well as the rotation speed and direction of the magnet. For example, when $d = 0$ and $r = 2.5$ mm, the MAC perform a vertical conical motion (VC motion, Figure 2d,f); and when $d = 6$ and $r = 6.5$ mm, the MAC perform a tilted conical motion (TC motion, Figure 2e,g,h). In the latter case, the MAC's motion cycle has an "effective stroke" when the cilium is mostly perpendicular to the surface, and a "recovery stroke" when the cilium is moving close to the floor (Figure 2e). As shown previously, a net fluid flow will be induced in the direction of the effective stroke.[8h] By rotating the ciliated pattern with respect to its own center while keeping the other parameters fixed, the direction of the effective stroke was varied between that normal to the edge of the ciliated square area (indicated as normal tilted cone, NTC, Figure 2g), and that inclined at a 45° angle to the edge (indicated as inclined tilted cone, ITC, Figure 2h). Since the MAC can bend with an average tilting angle of 72°,[8h] they can even touch their neighboring cilia, however the motion of the MAC is still uniform without any obvious interference (Figure 2g,h). This indicates the MAC have excellent magnetic properties and follow the applied magnetic field well, confirming the results of Zhang et al.[8h]

2.2. Particle-Removal Efficiency of Ciliated Surfaces

To characterize the particle-removal efficiency of the aforementioned ciliated surfaces, viscoelastic polylactic acid particles (PLA) with different mean diameters of 30, 100, 250, and 500 µm were used as representatives of fouling agents or microbeads. We chose PLA particles since they have a density close to that of water (1.1 to 1.5 g cm^{-3} according to the manufacturer), which is the case for most fouling agents such as the suspending marine biofouling agents.

2.2.1. Fully Ciliated Surface

Influence of MAC Motion and Actuation Frequency: We first investigated the impact of the MAC motion and the actuation frequency on the particle removal. The ciliated surface used here was a "fully ciliated surface" covered with the $10 \times 10 = 100$ MAC at a pitch of 250 µm, i.e., the total ciliated area was 5.29 mm^2, and the PLA particles had an average diameter of 100 µm.

Figure 3a shows snapshots of one recorded experiment (see Movie S1, Supporting Information) where the MAC performed the ITC motion at 40 Hz. Clearly, the vast majority of the particles were successfully removed from the ciliated area within a minute. The MAC are able to repel particles in their vicinity because they can induce local net flow and they can mechanically push the particles away by direct touch in the same direction as the local net flow (see Movie S2, Supporting Information). Consequently, the particles are repelled along the direction of the local net flow. Since the net flow direction beneath the cilia tips is in the same direction as the recovery stroke, and the net flow direction above the cilia tips is in the same direction as the effective stroke—the opposite direction of the recovery stroke, the particles located beneath the cilia tips are removed along the direction of the recovery stroke, and the particles suspended above the cilia tips or lifted up by the cilia are repelled along the opposite direction (see Movie S2, Supporting Information). Note that, the removed particles stayed on the surface around the ciliated area and could not be moved further by the flow generated by the cilia. Therefore, it was quite easy to collect them (for example, using a plastic pipette) and reuse them for further experiments. The calculated cleanness as a function of the actuation frequency for the aforementioned three different MAC motions (Figure 2f–h) is shown in Figure 3b. The cleanness is defined as $C_{60} = (N_0 - N_{60})/N_0$, where N_0 is the number of particles loaded in the ciliated area initially, and N_{60} is the number of particles left in the ciliated area after the MAC operating for 60 s. We chose 60 s because after that time there was almost no further change in the amount of particles within the ciliated area as shown in Figure 3c, in which the calculated cleanness is plotted as a function of the operating time of the MAC at different actuation frequencies when the MAC perform the ITC motion. The cleanness is now defined as $C_t = (N_0 - N_t)/N_0$, where N_0 is the number of particles within the ciliated area at time 0, and N_t is the number of particles left after the MAC operating for t seconds.

Observations from Figure 3b are: 1) the cleanness becomes better as the actuation frequency goes up, which means that the efficiency of the MAC in removing the particles is higher at a faster rotating frequency; 2) the TC motion is far more efficient than the VC motion; 3) the ITC motion slightly outperforms the NTC motion; and 4) over 95% of the particles can be eventually removed from the ciliated area when the MAC follow an ITC trajectory at 40 Hz, which creates an almost completely clean area.

Probable explanations for observation 1 are: a) at lower revolution frequencies, the net fluid flow induced by the MAC is smaller, and thus hydrodynamic forces acting on the particles are weaker and cannot overcome the adhesive forces between the particles and the PDMS walls, so that more particles remain stuck to the walls; b) the particles adhere to each other forming clusters that get stuck in between cilia, and the hydrodynamic forces at a
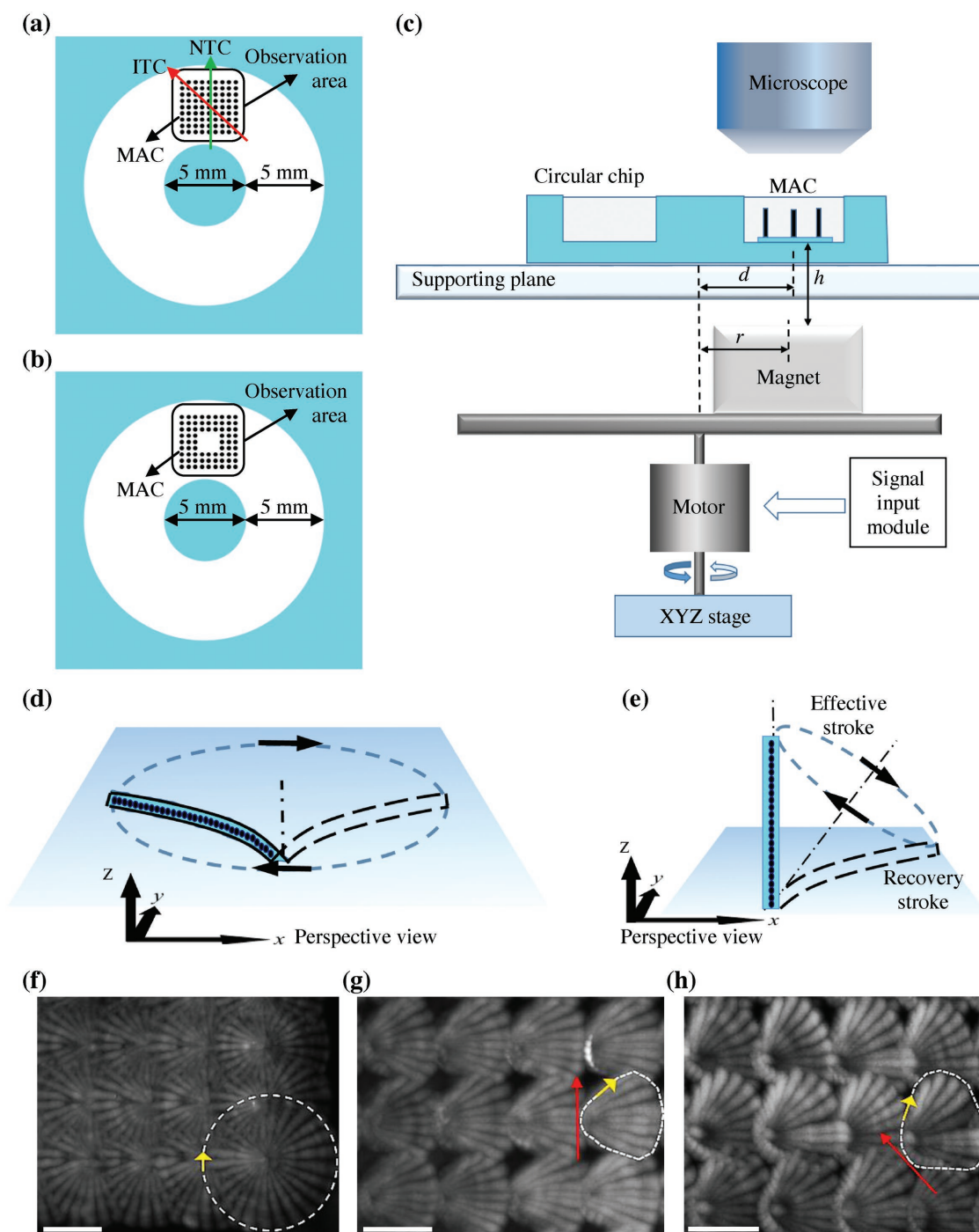
Figure 2. Actuation scheme and cilia motion. Schematic drawing of the open-top circular chip integrated with a) a fully ciliated surface and b) a partially ciliated surface, indicating the location of the ciliated surfaces and the observation area. The arrows NTC (normal tilted cone) and ITC (inclined tilted cone) indicate the direction of the effective stroke in case of the tilted conical motion of the MAC. The height of the chip is 4 mm. c–e) Actuation scheme of the fabricated MAC. c) Schematics of the actuation setup with MAC integrated in the circular chip, placed on a supporting plate and underneath a microscope. The rotation axis of the magnet is offset by a distance d with respect to the center of the ciliated area, and the magnet is placed at a distance r from the rotation axis. Reproduced with permission.[8h] Copyright 2018, Elsevier B.V. d) Schematic drawing of the rotating MAC performing a vertical conical motion in perspective view. e) Schematic drawing of the rotating cilium performing a tilted conical motion in perspective view. Illustrations are not to scale. Reproduced with permission.[8h] Copyright 2018, Elsevier B.V. Top-view images of the motion of the rotating MAC at 40 Hz in water showing f) the vertical cone (VC) rotation, g) the normal tilted cone (NTC) rotation, and h) the inclined tilted cone (ITC) rotation. Each image is composed of 25 overlapping frames in one actuation cycle. The white dashed lines indicate the cilia tip trajectories projected on the surface plane, the orange arrows indicate the rotation direction of the MAC, and the red arrows in (g) and (h) indicate the direction of the effective stroke. All scale bars are 250 µm.
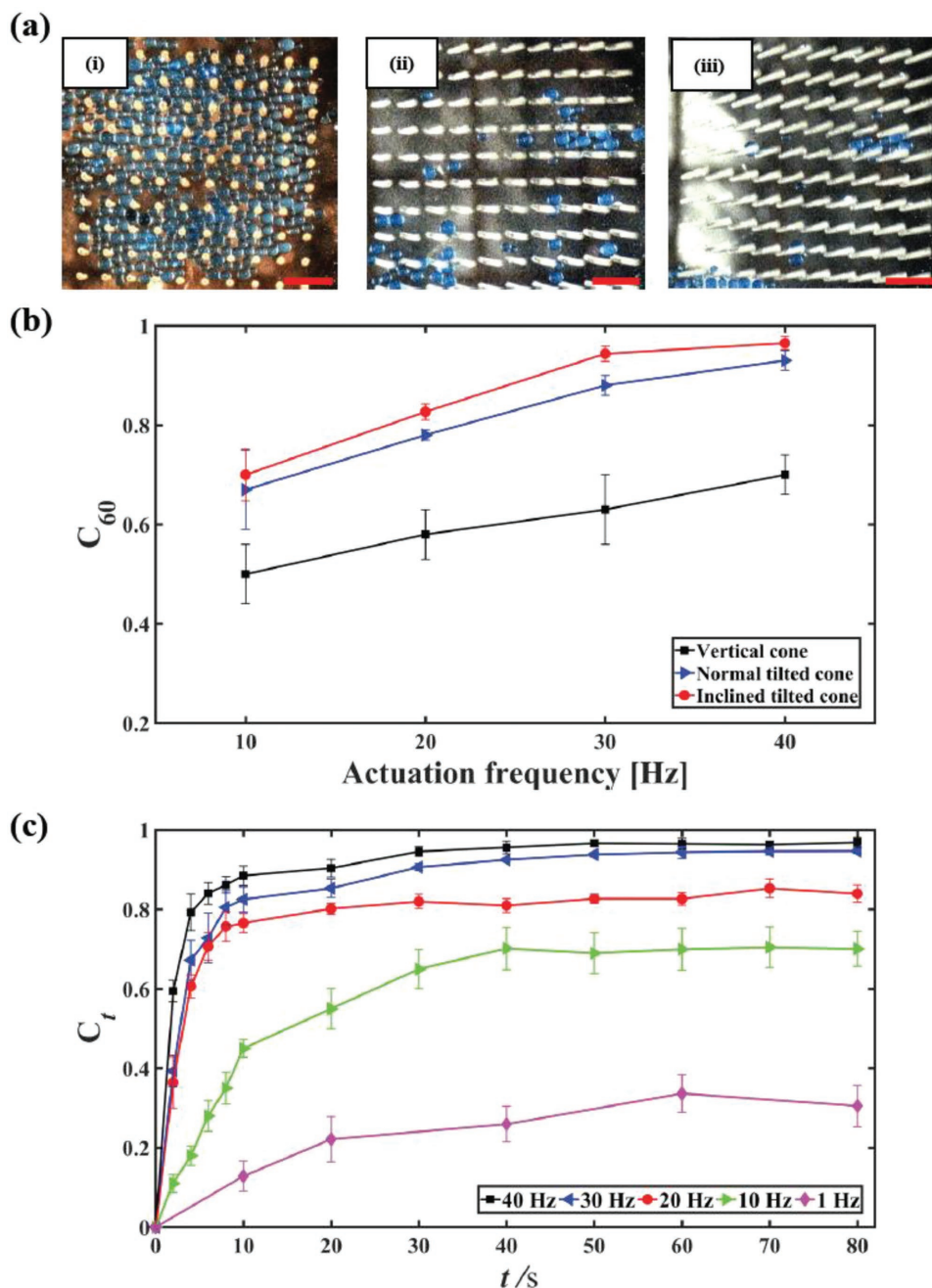
Figure 3. The influence of cilia motion and actuation frequency on the particle-removal efficiency. a) Snapshots from one recorded experiment after the MAC operate for i) 0 s (because the particles have a slightly larger density than water, they are all settled in between the MAC on the PDMS substrate initially), ii) 10 s, and ii) 1 min, showing that particles (blue) are gradually removed from the ciliated area. In this experiment, the MAC performed the ITC motion at 40 Hz; the microparticles had an average diameter of 100 μm. All scale bars are 500 μm. See also Videos S1 and S2 (Supporting Information). b) Calculated cleanness as a function of the actuation frequency for the three different MAC motions: VC, NTC, ITC motion, for the fully ciliated surface. The cleanness is defined as $C_{60} = (N_0 - N_{60})/N_0$, where N_0 is the number of particles within the ciliated area at time 0, and N_{60} is the number of particles after the MAC operating for 60 s. If C_{60} equals 1, no particle is left within the ciliated area. c) Calculated cleanness as a function of the operating time at different revolution frequencies of the MAC when the MAC perform the ITC motion. The cleanness is now defined as $C_t = (N_0 - N_t)/N_0$, where N_0 is the number of particles within the ciliated area at time 0, and N_t is the number of particles left after the MAC operating for t seconds. The error bars are the standard deviations of three identical but independent experiments. In these experiments, the MAC have a diameter of 50 μm, a height of 350 μm, and a pitch of 250 μm; the particles used are 100 μm spherical polylactic acid (PLA) particles.

lower actuation frequency are too weak to break these clusters, while the forces at a higher frequency are capable of breaking up the clusters and overcoming the adhesion between the particles and the PDMS walls. As to observation 2, possible reasons are: a) when the MAC perform the TC motion (NTC and ITC motion), a net flow is induced, which transports the particles continuously

**ADVANCED
SCIENCE NEWS**

www.advancedsciencenews.com

**ADVANCED
FUNCTIONAL
MATERIALS**

www.afm-journal.de

along one specific direction, and finally repels them from the ciliated area. However, when the MAC perform the VC motion, no net flow can be generated over one rotating cycle resulting in relatively low cleanness; and the removed particles are likely a result from the mechanical pushing by the cilia (see Movie S3, Supporting Information); b) in one rotation cycle of the VC motion, individual particles are pushed to one side by one cilium during the first half cycle, while they are subsequently pushed back by the neighboring cilium during the second half, and the particles barely move in a full cycle (see Movie S3, Supporting Information). Regarding observation 3, plausible explanations are: a) when the MAC perform the ITC motion, the swept area by the cilia is larger because neighboring cilia have less interference with each other (see Figure 2g,h)—this means that effectively, the generated flow speed and consequent hydrodynamic forces acting on the particles are larger for the ITC motion; b) less particles reenter the ciliated area when the MAC perform the ITC motion since particles are repelled further away from the ciliated area, while for the NTC motion, the repelled particles remain close to the ciliated area; this seems to be a result of the local flow profile: the flow is parallel to the edge of the ciliated area for the NTC motion, and the flow is along the diagonal of the ciliated area for the ITC motion. Regarding observation 4: even though the cleanness is high, it is not 100%, which is probably because a) some particle clusters are too strong to be broken up at an actuation frequency of 40 Hz; b) the hydrodynamic forces cannot overcome the adhesion forces between some of the particles and the PDMS walls. Tuning the surface energy of the walls and the cilia with respect to the particles, and/or applying a higher actuation frequency than 40 Hz will lead to a better cleanness, and this work is still ongoing.

Observations from Figure 3c are: 1) the cleanness is better for a higher actuation frequency; 2) the time needed to reach the final cleanness is shorter for a higher actuation frequency, and the cleanness reaches 90% within 10 s when the MAC rotate at 40 Hz. The explanations for the frequency dependence are the same as those for observation 1 from Figure 3b. The probable reason for the time dependence is that both the MAC velocity and the generated net fluid flow velocity are higher at higher frequencies, and therefore the particles move faster through and out of the ciliated area due to the higher direct and hydrodynamic forces acting on them.

Influence of Particle Size and Cilia Pitch: As Figure 3b shows that the obtained cleanness is the best when the MAC perform the ITC motion at 40 Hz using PLA particles of 100 μm in diameter, we, subsequently, studied whether the "fully ciliated surface" was also capable of removing PLA particles of different sizes at the same actuation condition while altering the cilia pitch from 250 to 350 and to 450 μm. The different PLA particles used here had an average diameter of 30, 100, 250, and 500 μm, respectively. **Figure 4**a shows some examples of these experiments. The calculated cleanness as a function of the ratio between the particle diameter and the cilia pitch is plotted in Figure 4b, where the cleanness is again defined as $C_{60} = (N_0 - N_{60})/N_0$. It is clear that 1) the "fully ciliated surface" can remove over 95% of the particles that have a diameter over 1.1 times the cilia pitch, and especially all the particles that have a size larger than 1.4 times of cilia pitch are removed; 2) the cleanness is less than 40% when the particles have a diameter equal to the cilia

pitch, which is the worst situation; 3) the surface has the capacity to remove over 80% of the particles with a diameter between 0.1 and 0.8 times the cilia pitch; and 4) when particle size to cilia pitch ratio goes even smaller, the cleanness becomes worse.

As to observation 1, the particles much larger than the cilia pitch remain on top of the cilia since they cannot enter the space between the cilia, and the ciliated surface repels all of them in the direction of the effective cilia stroke by periodical direct push as is shown in the recorded videos (see Movie S4, Supporting Information). When the particles have an average diameter (500 μm) of 1.1 times the cilia pitch (450 μm), they can still go in between cilia because their size is smaller than the diagonal distance between cilia. But the particles are taller than the cilia, so they do not inhibit the cilia motion. On the contrary, they can be mechanically pushed by the cilia easily (see Movie S5, Supporting Information). Consequently, almost no particle is left in the ciliated area.

Regarding observation 2, when the particles' diameter is the same as the cilia pitch, they get stuck in between cilia, and their presence restrains the motion of the cilia, resulting in decreased net local flow and hence lower hydrodynamic forces (see Movie S6, Supporting Information). Regarding observation 3, because the particles are smaller than the cilia pitch, they seldom get stuck in between cilia; and due to both the direct cilia push and hydrodynamic forces induced by the cilia rotation, over 80% of the particles are removed. Nevertheless, some residual particles get stuck in the ciliated area. This is probably because a) the hydrodynamic forces cannot overcome the adhesion forces between the particles and the PDMS walls; b) the particles form clusters, and the forces induced by the MAC acting on the clusters in the form of either direct touch or hydrodynamic forces are too weak to break up the clusters, and/or c) the particles are "trapped" within recirculating flows occurring within the ciliated area (see Movie S7, Supporting Information). The possible reasons for observation 4 are as follows. First, considering the no-slip boundary condition, the actual flow speed closer to the bottom of the channel is smaller and, therefore, at the same condition, the hydrodynamic forces acting on a smaller particle sitting on the bottom is smaller. Second, more particles are trapped in the local recirculating flows.

We expect the cleanness to be worse when particle size still goes smaller than 0.06 times the cilia pitch. In order to remove such small or even smaller particles, MAC arrays with smaller size and pitch should be used. This will be a subject of our future research. We expect that the cleanness will remain 1 when the particle size goes larger than two times the cilia pitch.

Removal of Sand Grains: In order to show the versatility of the ciliated surface, we repeated the experiments using real sand grains instead of the PLA particles. The sand was obtained from the field, and they had irregular shapes and sizes (the dimension is from 0.5 to 2 mm) much larger than the cilia pitch (see **Figure 5** and Movie S8, Supporting Information). The MAC had a diameter of 50 μm, a height of 350 μm and a pitch of 250 μm. The results show that all sand can be removed from the ciliated area even though they are much heavier than water (the average density of the sand is approximately 1.6 g cm^{-3} calculated by measuring the weight and volume). Notably, even when no liquid is added into the channel, the sand can still be removed. In other words, the cilia have the capacity to remove sand in air.
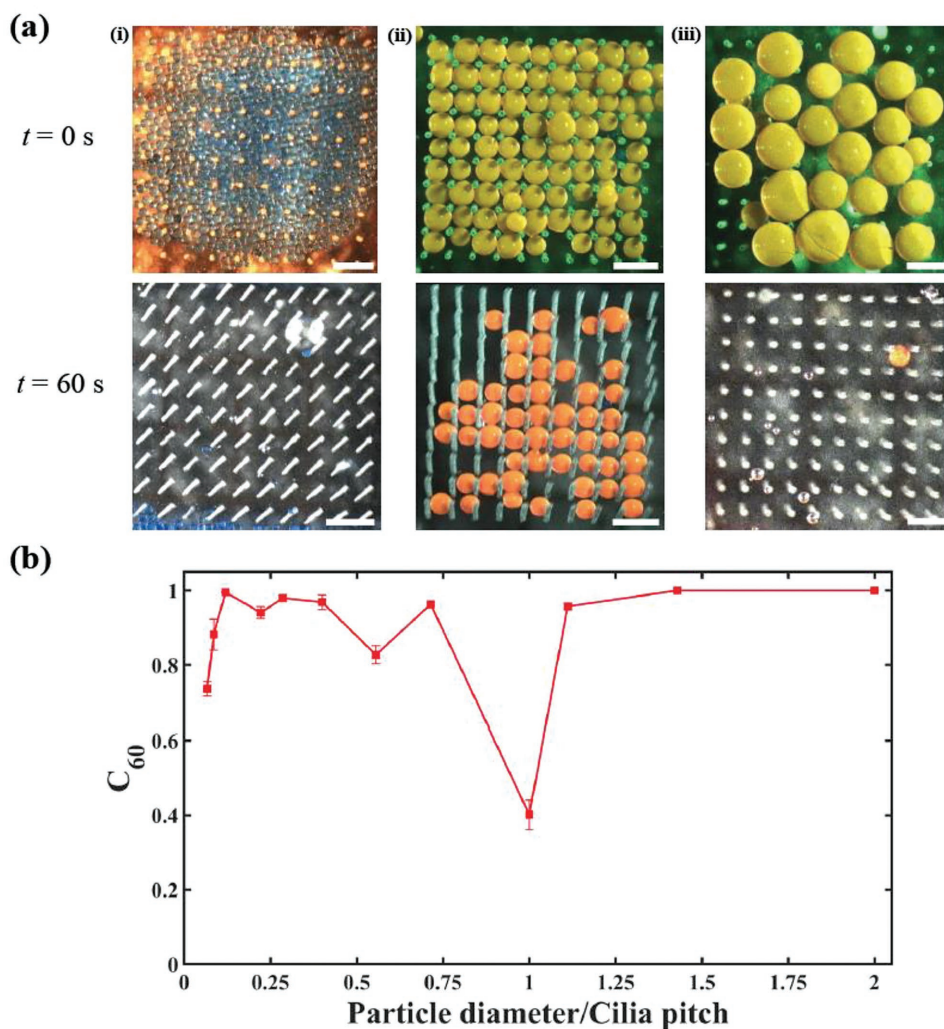
ADVANCED
SCIENCE NEWS
www.advancedsciencenews.com

ADVANCED
FUNCTIONAL
MATERIALS
www.afm-journal.de

Figure 4. The influence of particle size and cilia pitch on the particle-removal efficiency for the fully ciliated area. a) Snapshots from the recorded experiments for particle size to cilia pitch ratio of i) 2/7 (the particle size is 100 µm and the cilia pitch is 350 µm), ii) 1 (both the particle size and the cilia pitch are 250 µm; note that because of optical effect the particles exhibit different colors at different time points), and iii) 2 (the particle size is 500 µm and the cilia pitch is 250 µm). The scale bars in (i) are 700 µm, and the scales bars in (ii) and (iii) are 500 µm. b) Calculated cleanness as a function of the ratio between the particle diameter and the cilia pitch when the MAC perform the ITC motion at 40 Hz for the fully ciliated surface. The cleanness is $C_{60} = (N_0 - N_{60})/N_0$. The error bars are the standard deviations of three identical experiments.

Figure 5. Removal of real sand grains by magnetic artificial cilia. Snapshots from one recorded experiment after the MAC operate for a) 0 s (because the sand grains have a larger size than the cilia pitch, they all settle on top of the cilia tips initially), b) 16 s, and c) 30 s, showing that all sand grains are gradually removed from the ciliated area. In this experiment, the MAC performed the ITC motion, and the rotating speed was initially 0.1 Hz and was then suddenly increased to 40 Hz. All scale bars are 1 mm. See also Video S8 (Supporting Information).

2.2.2. Partially Ciliated Surface

We have demonstrated that the "fully ciliated surface" is able to almost completely remove a large size range of particles. In this section, we study the capability of the "partially ciliated surface" shown in Figure 1b to remove particles. The application of this configuration might be to keep clean a sensor surface located in the unciliated region. The MAC have a constant pitch

of 250 µm and perform the ITC motion at 40 Hz in all experiments reported in this section.

Influence of the Size of the Unciliated Region: We first studied the capacities of the "partially ciliated surface" with a variable unciliated central region by changing the number of "removed" cilia: first, 1 cilium at the center was removed, which resulted in an unciliated area of 0.25 mm² (**Figure 6**a); second, 16 cilia were removed, with an unciliated area of 1.56 mm² (Figure 6b);
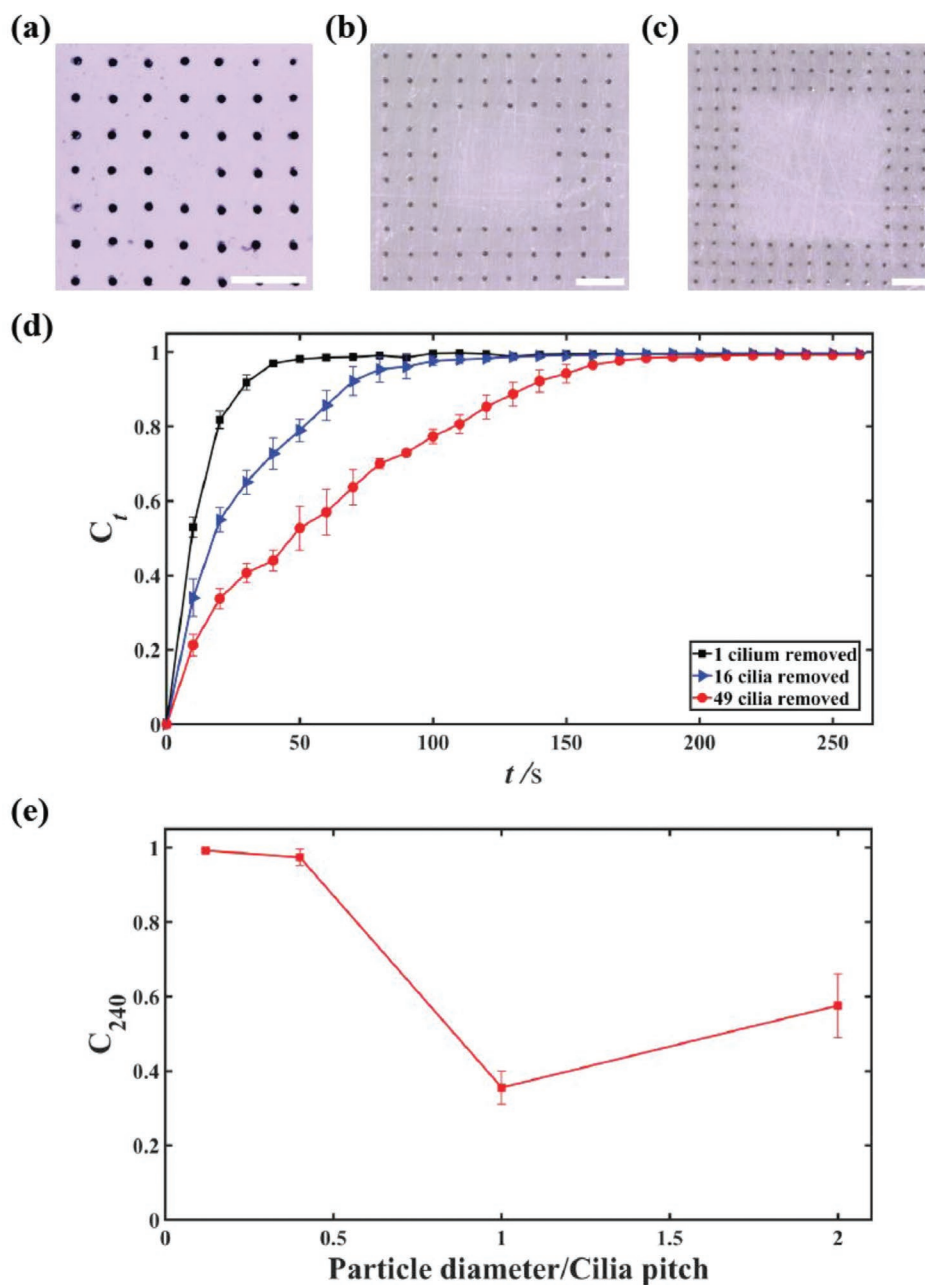

Figure 6. Top-view optical microscopy images of the three types of "partially ciliated surfaces": a) one cilium is removed, b) 16 cilia are removed, and c) 49 cilia are removed. All scale bars are 500 µm. d) Calculated cleanness as a function of the working time for the three types of "partially ciliated surfaces." The cleanness is defined as $C_t = (N_0 - N_t)/N_0$. The error bars are the standard deviation of three experiments. The particles are 30 µm PLA particles. e) Calculated cleanness for the partially ciliated surface with 49 cilia removed as a function of the ratio between the particle diameter and the cilia pitch when the MAC perform the ITC motion at 40 Hz, for a duration of 240 s. The cleanness is determined after 240 s: $C_{240} = (N_0 - N_{240})/N_0$. The error bars are the standard deviations of three experiments. In these experiments, the MAC have a diameter of 50 µm, a height of 350 µm, and a pitch of 250 µm.

1806434 (8 of 11)

**ADVANCED
SCIENCE NEWS**
www.advancedsciencenews.com

**ADVANCED
FUNCTIONAL
MATERIALS**
www.afm-journal.de

and third, 49 cilia were removed, having an unciliated central area of 4 mm^2 (Figure 6c). The particles used here are 30 μm PLA particles. The calculated cleanness as a function of the operational time for these three types of surfaces is depicted in Figure 6d. The cleanness is now defined as $C_t = (N_0 - N_t)/N_0$, in which N_0 is the number of particles within the unciliated central area at time 0, and N_t is the number of particles left in the central area after the MAC operating for t seconds. There are two observations: 1) the final cleanness is the same for all three types of "partially ciliated surfaces," and it is almost 100%, i.e., all central regions are "cleaned" almost perfectly (see Movie S9, Supporting Information); 2) the time needed to reach the final cleanness is shorter for a surface with less cilia removed. Regarding the observation 1, the hydrodynamic forces acting on the particles to overcome the particle-surface adhesion strength and to propel the particles is sufficient to remove almost all particles for all three types of "partially ciliated surfaces," even though they are smaller for a surface with a larger unciliated central area. If the surface is not 100% clean, this is probably a result of particle reentrance into the central area. The possible reasons for the observation 2 are as follows. First of all, for a "partially ciliated surface" with a smaller unciliated central area, the local flow generated by the rotating MAC within that area is stronger, and thus hydrodynamic forces acting on the particles are stronger. Second, more particles are within the touching range of the cilia for a "partially ciliated surface" with a smaller unciliated central area.

We expect that it will take more time to reach the final state and that the final cleanness will become worse if the unciliated central area becomes even larger. Most importantly, we have demonstrated that a ciliated surface with a central unciliated area of up to 4 mm^2 is capable of removing virtually all 30 μm particles, creating a completely clean area.

Influence of Particle Size: In the previous section we have demonstrated that the "partially ciliated surface" is capable of removing 30 μm particles. Will it also be able to remove particles of different sizes just like the "fully ciliated surface" did? To answer this question, we performed experiments using the "partially ciliated surface" with 49 cilia removed and PLA particles with average diameters of 30, 100, 250, and 500 μm, respectively. The calculated cleanness as a function of the operational time for different particle sizes is plotted in Figure 6e. The cleanness is now determined after 240s of operation, as $C_{240} = (N_0 - N_{240})/N_0$. The results show some similarities to Figure 4b. The cleanness is the worst when the particle size is equal to the cilia pitch. The cleanness is over 90% when the particle diameter is smaller than 1/2 the cilia pitch; specifically, the cleanness is better for a smaller particle size. However, the cleanness is around 50% when the particle diameter is twice the cilia pitch for the partially ciliated area, which is substantially lower than for the fully ciliated area (Figure 4b). The probable reasons are as follows. First, the particles with a diameter equal to or larger than the cilia pitch cannot pass between the cilia, through the "cilia wall," and only a few of them can be expelled by direct cilia touch. Second, despite that 100 μm particles are smaller than the cilia pitch, they can form clusters that are larger than the cilia pitch, and hence cannot pass between the cilia. A video illustrating the removal of the 100 μm particles can be found in the Movie S10 (Supporting Information).

We expect that a "partially ciliated surface" featured with cilia with a pitch larger than 500 μm is able to repel the majority of 250 and 500 μm particles from the unciliated central region as well, and that when the particles become even smaller than 30 μm, the cleanness will decrease at some critical value, for then the hydrodynamic forces acting on the particles will not be able to overcome the adhesion forces between the particles and the PDMS substrate.

3. Conclusions and Outlook

For the first time, we have experimentally proven that MAC can remove microparticles and sand from the ciliated surface area. We have shown this for two configurations, namely a surface region fully covered with orthogonally arranged MAC, the "fully ciliated surface," and a bare unciliated central region surrounded by rows of MAC, the "partially ciliated surface." The fully ciliated surface is able to remove the vast majority of a large size range (30 to 500 μm) of microparticles when the MAC, with a diameter of 50 μm, a length of 350 μm, and a pitch between 250 and 450 μm, perform the ITC motion at 40 Hz. The cleanness can reach 100% if the particles are too large to enter the space between the cilia. Only particles with a diameter equal to or much smaller than the cilia pitch cannot be easily removed. Note that, particles that stay above the cilia tips are repelled in the direction of the effective stroke, and particles that entered the ciliated area are removed along the direction of the recovery stroke. This shows that the direction of removal of particles can in principle be controlled, which means that the concept may be used for particle accumulation, sorting and collecting. Additionally, the fully ciliated surface can remove all irregular-shaped sand grains in both water and air. The partially ciliated surface has the capacity to remove over 99% of particles from the central unciliated region, creating an almost completely clean area, for unciliated areas at least as large as 4 mm^2. Importantly, we did not observe any breaking or rupturing of the MAC within the time duration of the experiments that continued for approximately one month, nor any other degradation of their functionality, which clearly proves that our MAC are mechanically robust. As presented in the Supporting Information, besides the particle-removal capability, the MAC are also demonstrated to be capable of preventing particles from entering the ciliated area in the first place, i.e., "particle exclusion." This research offers a new method to manipulate microparticles and to create a novel type of self-cleaning/anti-fouling surface, which can find applications in, for example, 1) particle or cell manipulation for lab-on-a-chip devices where microscale analyses of particulates are performed[10]; 2) anti-fouling of water-submerged surfaces, such as marine sensors,[2] water quality analyzers, etc. Note that, when a rotating magnet is inaccessible, electrostatic field,[8a] electromagnetic field,[8e,f] resonance,[8i,m] pneumatic pressure,[8n] and even ambient flow[9h,i] can serve as alternatives.

Our results provide a first experimental proof-of-principle of the particle manipulation effects by active cilia, but toward applications more research and technological development need to be done. One of the issues for antifouling applications is our use of PDMS which is known as a material very easily

contaminated by small molecule absorption and adsorption. However, Amini et al. have shown that silicone oil infused PDMS is very effective to prevent the adhesion of mussel,[11] which offers a possible solution for this problem. So one topic of future research therefore should be the use of lubricate-infused PDMS or alternative materials. Related to this, particle-cilia and particle-surface adhesion are important; in our experiments we have lowered adhesion by adding sodium dodecyl sulfonate (SDS) to the fluid. In the future, we will address this topic further by tuning surface energy of the cilia and the substrate surface in a more controlled manner, to modify particle-cilia and particle-surface adhesion and quantitatively study its effect on particle manipulation. Also, for practical applications, it is important to study the possibility of manipulation of even smaller particles than we used here (i.e., smaller than 30 μm); this will require further miniaturization of the MAC, possibly down to the size of biological cilia (namely about 10 μm long). Also, our experiments were all done with PLA particles and for practical applications other types of particles (e.g., nonviscoelastic) should be tested too. In addition, toward applications, testing in practically relevant circumstances (e.g., at different temperatures or in fluids with varying salinity) should be subject of future research. Finally, although active cilia are desirable to actively manipulate particulates, active actuation may not be achievable in some practical situations (e.g., in applications to ship hulls). Therefore, our future work also includes the study of the antifouling property of passive cilia (simply moved by external flow) based on the findings in this article.

4. Experimental Section

Fabrication of MAC: The MAC used in this article were the so-called LAP MAC (MAC with linearly aligned magnetic particles along the cilia's long axis) reported in our previous study.[8h] The fabrication process of the MAC can be summarized as follows (Figure 1c): (1) A mold featured with microwells was fabricated using standard photolithography. 2) A uniform precursor mixture of polydimethylsiloxane (PDMS, the Base to Curing Agent weight ratio is 10:1) and superparamagnetic microparticles (Carbonyl iron powder, CIP, 99.5%, SIGMA-ALDRICH) was poured onto the mold, followed by a degassing procedure. 3) The top layer of the PDMS-CIP mixture was removed. 4) Pure PDMS was poured onto the mold. After degassing the pure PDMS layer was defined to a thickness of 100 μm by spin-coating at a rotating speed of 500 rpm for 50 s. 5) A permanent magnet with a size of $15 \times 15 \times 8$ mm^3 and a remnant flux density of 1.2 T was put underneath the mold in order to align the magnetic particles within the mold. The sample was left in an oven at 80 °C for 2 h to cure the mixture. 6) The cured pure PDMS layer with PDMS-CIP micropillars was peeled off the SU-8 mold. Finally, the MAC with the same geometry as the mold, namely a diameter of 50 μm and a height of 350 μm, were obtained, "standing" on a transparent PDMS base substrate.

Magnetic Actuation Setup: The homebuilt magnetic actuation setup (see Figure 2c) was comprised of a manual linear XYZ translational stage at the bottom, an electric motor in the middle, an offset magnet mounted on the motor, and a safety box containing the supporting plane (a transparent glass plate of thickness of 1.5 mm) on top of which the chip containing the MAC could be placed. The magnet, which had a geometry of $20 \times 20 \times 10$ mm^3 with a remnant flux density of 1.3 T, was positioned at an offset *r* with respect to its rotation axis which is again offset by *d* with respect to the center of the ciliated area.

Methods to Measure the Removal of Microparticles: In this paper, viscoelastic PLA (plain, micromod Partikeltechnologie GmbH) with different mean diameters of 30, 100, 250, and 500 μm were used as representatives of fouling agents or microbeads. The particle removal experiments were performed in the following way. First, the highly concentrated particles in deionized water were loaded into the ciliated area using a plastic pipette, at a particle concentration which assured that approximately only one layer of particles was covering the ciliated surface. The locations of the ciliated surfaces are indicated in Figure 2a,b which also show the observation area of the experiments. Then, an SDS solution (0.1 vol%) was injected slowly into the circular chip indicated in Figure 2a,b to completely fill the channel using a plastic pipette. The purpose of using SDS solution instead of pure deionized water is to reduce the adhesion between the particles and the PDMS (see the Supporting Information). Because the particles have a slightly larger density than water, the particles that are too large to enter the ciliated area did settle on top of the ciliated surface, and the particles that can enter the ciliated area did settle on the PDMS substrate initially (see Figure 3a). Subsequently, during experiments, the MAC were actuated by the magnetic setup (Figure 2c). A high-speed camera (Phantom V9) mounted on a stereo microscope was used to capture the movement of the MAC and the particles from right above by taking image sequences at a frame rate of 1000 fps when the actuating magnet was rotating at a frequency of 40 Hz. And, separately, a CMOS camera (The Imaging Source Europe GmbH) mounted on the stereo microscope was used to record the distribution of the particles by taking image sequences at a frame rate of 60 fps. Finally, the number of particles left in the ciliated area was counted using the image analyzing software ImageJ. Each data point was obtained by averaging the results of three identically performed experiments. In some of the experiments, tracer particles were added to the fluid (5 μm polystyrene particles, white color, micromod Partikeltechnologie GmbH) to study qualitatively the fluid flow generated by the cilia (visible in some of the movies in the Supporting Information).

Supporting Information

Supporting Information is available from the Wiley Online Library or from the author.

Conflict of Interest

The authors declare no conflict of interest.

[1] a) M. Wahl, *Mar. Ecol. Prog. Ser.* **1989**, *58*, 175; b) P. Schultz, *Biofouling* **2007**, *23*, 331; c) E. S. Poloczanska, A. J. Butler, *Biofouling and Climate Change*, Wiley-Blackwell, Oxford, UK **2010**;

d) M. P. Schultz, J. A. Bendick, E. R. Holm, W. M. Hertel, *Biofouling* **2011**, *27*, 87; e) M. Otani, T. Oumi, S. Uwai, T. Hanyuda, R. E. Prabowo, T. Yamaguchi, H. Kawai, *Biofouling* **2007**, *23*, 277; f) T. Yamaguchi, R. E. Prabowo, Y. Ohshiro, T. Shimono, D. Jones, H. Kawai, M. Otani, A. Oshino, S. Inagawa, T. Akaya, I. Tamura, *Biofouling* **2009**, *25*, 325; g) J. B. Pettengill, D. E. Wendt, M. D. Schug, M. G. Hadfield, *Biofouling* **2007**, *23*, 161; h) R. F. Piola, E. L. Johnston, *Biofouling* **2008**, *24*, 145; i) R. Mukhopadhyay, *Anal. Chem.* **2005**, *77*, 429 A.

[2] L. Delauney, C. Compère, M. Lehaitre, *Ocean Sci.* **2010**, *6*, 503.

[3] a) C. M. Kirschner, A. B. Brennan, *Annu. Rev. Mater. Res.* **2012**, *42*, 211; b) J. A. Callow, M. E. Callow, *Nat. Commun.* **2011**, *2*, 244; c) L. D. Chambers, K. R. Stokes, F. C. Walsh, R. J. K. Wood, *Surf. Coat. Technol.* **2006**, *201*, 3642.

[4] a) M. Sleigh, *Comp. Biochem. Physiol., Part A: Mol. Integr. Physiol.* **1989**, *94*, 359; b) Y. Enuka, I. Hanukoglu, O. Edelheit, H. Vaknine, A. Hanukoglu, *Histochem. Cell Biol.* **2012**, *137*, 339; c) L. J. Fauci, R. Dillon, *Annu. Rev. Fluid Mech.* **2006**, *38*, 371; d) H. U. Riisgard, P. S. Larsen, *Limnol. Oceanogr.* **2001**, *46*, 882; e) R. R. Strathmann, T. L. Jahn, J. Fonseca, *Biol. Bull.* **1972**, *142*, 505; f) M. LaBarbera, *J. Exp. Mar. Biol. Ecol.* **1981**, *55*, 185; g) M. LaBarbera, *Am. Zool.* **1984**, *24*, 71; h) G. L. Taghon, *Oecologia* **1982**, *52*, 295; i) P. A. Jumars, R. F. L. Self, A. R. Nowell, *J. Exp. Mar. Biol. Ecol.* **1982**, *64*, 47; j) M. R. Romero, H. C. P. Kelstrup, R. R. Strathmann, *Biol. Bull.* **2010**, *218*, 145; k) L. W. Fritz, R. A. Lutz, M. A. Foote, C. L. Van Dover, J. W. Ewart, *Estuaries* **1984**, *7*, 513; l) M. Wahl, K. Kröger, M. Lenz, *Biofouling* **1998**, *12*, 205; m) E. E. Ruppert, R. S. Fox, R. B. Barnes, *Invertebrate Zoology*, Brooks Cole Thomson, Belmont, CA, **2004**; n) M. G. Stafford-Smith, R. F. G. Ormond, *Mar. Freshwater Res.* **1992**, *43*, 683.

[5] D. Clifford, *Antony van Leeuwenhoek and His "Little Animals,"* Russel & Russel Publishers, New York **1932**.

[6] J. den Toonder, P. R. Onck, *Artificial Cilia*, RSC Publishing, Cambridge **2013**.

[7] J. R. Blake, M. A. Sleigh, *Bio. Rev.* **1974**, *49*, 85.

[8] a) J. den Toonder, F. Bos, D. Broer, L. Filippini, M. Gillies, J. de Goede, T. Mol, M. Reijme, W. Talen, H. Wilderbeek, V. Khatavkar, P. Anderson, *Lab Chip* **2008**, *8*, 533; b) J. den Toonder,

P. Onck, *Trends Biotechnol.* **2013**, *31*, 85; c) S. Khaderi, C. Craus, J. Hussong, N. Schorr, *Lab Chip* **2011**, *11*, 2002; d) S. Khaderi, J. Hussong, J. Westerweel, J. den Toonder, P. Onck, *RSC Adv.* **2013**, *3*, 12735; e) Y. Wang, Y. Gao, H. Wyss, P. Anderson, J. den Toonder, *Lab Chip* **2013**, *13*, 3360; f) Y. Wang, Y. Gao, H. M. Wyss, P. D. Anderson, J. den Toonder, *Microfluid. Nanofluid.* **2015**, *18*, 167; g) Y. Wang, J. den Toonder, R. Cardinaels, P. Anderson, *Lab Chip* **2016**, *16*, 2277; h) S. Zhang, Y. Wang, R. Lavrijsen, P. R. Onck, J. den Toonder, *Sens. Actuators, B* **2018**, *263*, 614; i) K. Oh, B. Smith, S. Devasia, J. J. Riley, J. H. Chung, *Microfluid. Nanofluid.* **2010**, *9*, 645; j) C.-Y. Chen, C.-Y. Chen, C.-Y. Lin, Y.-T. Hu, *Lab Chip* **2013**, *13*, 2834; k) C. L. van Oosten, C. W. M. Bastiaansen, D. J. Broer, *Nat. Mater.* **2009**, *8*, 677; l) L. D. Zarzar, P. Kim, J. Aizenberg, *Adv. Mater.* **2011**, *23*, 1; m) K. Oh, J. H. Chung, S. Devasia, J. J. Riley, *Lab Chip* **2009**, *9*, 1561; n) B. Gorissen, M. de Volder, D. Reynaerts, *Lab Chip* **2015**, *15*, 4348; o) S. Hanasoge, P. J. Hesketh, A. Alexeev, *Microsyst. Nanoeng.* **2018**, *4*, 11; p) S. Khaderi, P. Onck, J. den Toonder, *J. Fluid Mech.* **2011**, *688*, 44; q) S. Khaderi, M. Baltussen, P. D. Anderson, J. den Toonder, P. Onck; *Phys. Rev. E* **2010**, *82*, 027302.

[9] a) R. Ghosh, G. A. Buxton, O. B. Usta, A. C. Balazs, A. Alexeev, *Langmuir* **2010**, *26*, 2963; b) A. Bhattacharya, G. A. Buxton, O. B. Usta, A. C. Balazs, *Langmuir* **2012**, *28*, 3217; c) A. Tripathi, A. Bhattacharya, A. C. Balazs, *Langmuir* **2013**, *29*, 4616; d) A. Bhattacharya, A. C. Balazs, *Soft Matter* **2013**, *9*, 3945; e) H. Shum, A. Tripathi, J. M. Yeomans, A. C. Balazs, *Langmuir* **2013**, *29*, 12770; f) P. Dayal, O. Kuksenok, A. Bhattacharya, A. C. Balazs, *J. Mater. Chem.* **2012**, *22*, 241; g) A. C. Balazs, A. Bhattacharya, A. Tripathi, H. Shum, *J. Phys. Chem. Lett.* **2014**, *5*, 1691; h) A. Tripathi, H. Shum, A. C. Balazs, *Soft Matter* **2014**, *10*, 1416; i) J. Branscomb, A. Alexeev, *Soft Matter* **2010**, *6*, 4066; j) H. Masoud, A. Alexeev, *Soft Matter* **2011**, *7*, 8702; k) J. H. Kim, S. M. Kang, B. J. Lee, H. Ko, W. Bae, K. Y. Suh, M. K. Kwak, H. E. Jeong, *Sci. Rep.* **2016**, *5*, 17843; l) Z. Yang, J. K. Park, S. Kim, *Small* **2018**, *14*, 1702839.

[10] D. Huh, W. G. Y. Kamotani, J. B. Grotberg, S. Takayama, *Physiol. Meas.* **2005**, *26*, R73.

[11] S. Amini, S. Kolle, L. Petrone, O. Ahanotu, S. Sunny, C. N. Sutanto, S. Hoon, L. Cohen, J. C. Weaver, J. Aizenberg, N. Vogel, A. Miserez, *Science* **2017**, *357*, 668.